INTELLIGENT SPATIAL OBJECT DIGITIZATION BASED ON STEREO IMAGES

Keywords: close range photogrammetry, 3D surface reconstruction, 3D triangular mesh, adaptive pattern projection, iterative reconstruction, surface curvature.

Abstract: In computer vision, active stereoscopic systems are widely used for 3D surface reconstruction of real objects. Many structured light approaches have been shown in the literature. However, not anyone adapted the processing to the geometrical characteristics of the surface. Instead, the sensing process covers uniformly the entire object in order to obtain a very dense 3D point cloud. A further time-consuming mesh simplification task is therefore necessary to simplify the manipulation of the 3D model. This could be avoided, if the sensing process is already as intelligent as necessary to generate only those points needed to optimally describe the surface. In our development we show a solution, which is based on an iterative process adapting the point distribution to the spatial structure of the object. Starting from an initial sparse point pattern a refinement process is guided which analyses the object based on curvature measurements allowing to detect areas of greater morphological variation where further measurements have to be introduced. Thus, the acquired 3D model is already optimised during the acquisition process. Numerous experiments showed that compared to the 3D models generated from commercial system, the loss of morphological quality is negligible, but the gain by the simplification of the model is considerable.

1. INTRODUCTION

In 3D reconstruction field, Close Range Photogrammetry is an often used technique. The users of Close Range Photogrammetry can be: Architects and civil engineers (to supervise buildings, document their current state, deformations or damages), industrial Quality control, archaeologists surgeons (plastic surgery), police departments (documentation of traffic accidents and crime scenes), etc.

Depending on the available material and the required results, different photogrammetric techniques can be applied, among which stereophotogrammetry is a simple and effective one. As the term implies, stereophotogrammetry uses stereopair as the basic equipment. A stereopair can be produced with a single camera which takes pictures from two different positions, or by using two metric cameras which are fixed at two known positions. The 3D reconstruction system which uses stereophotogrammetry technique is named as “stereoscopic system”.

Stereoscopic system can be divided into two categories: passive and active. In passive stereoscopic systems, image rays are identified by using the texture available on the surface. For objects with low texture information, the identification of the image rays becomes very difficult. In active systems, a projector creates a synthetic texture on the surface of the object, which simplifies the identification of image rays, thus the rate of detected object points can be highly increased.

Most of the current active systems ignore the geometrical structure of the surface of the object. Such approaches are necessary for objects with very complicated surface. However, for those with relatively simple surface geometry, the reconstructed 3D model can contain large number of useless data which describes a flat or nearly flat area, and it can easily reach to a size of gigabytes. The sheer amount of data not only exhausts the main memory resources of common desktop PCs, but also exceeds the 4 gigabyte address space of 32-bit machines; it makes the subsequent processing difficult (ex., save, transmission, rendering, etc.). Therefore, the further mesh simplification is often necessary.

In this paper, we present a new concept which is based on an automatic and adaptive projection strategy. The reconstruction process begins by projecting a regular spot pattern to get a rough initial 3D surface model. The Local Surface Curvature (LSC) of the actual reconstructed 3D surface is estimated after each iteration, and for the next iteration, a new pattern is created according to the LSC of each reconstructed 3D point. Thus the reconstructed 3D surface is refined progressively. The final reconstructed 3D model was proved to be optimized: compared to the 3D model obtained by traditional solutions, the number of points was largely reduced, whereas all important morphological information of the object was captured (Interested readers can refer to [1] for more details about mesh optimization). This concept was at first validated by simulated data [2]. In this paper, we focus on the final real-time system which works on real objects.

The remainder of this article is organized as follows: section 2 presents the 3D reconstruction process; section 3 presents some results and discussion; finally, we conclude and show perspectives in section 4.

2. 3D RECONSTRUCTION PROCESS

The spatial reconstruction is based on two metric cameras and a projection device, which are directed to the surface to be captured. In principle every digital camera can be used, it only has to be assured, that the internal camera geometry is known. This can be achieved by a calibration process which has to be undertaken prior to the data capture. In addition, all devices have to be known in their spatial relations, which can be assured by a further orientation step. All these steps are provided in the software package and have to be applied appropriately.

Once the system is calibrated, the 3D reconstruction process can be carried out. The objective of the processing is to obtain a 3D model represented by a minimum number of points, whereas it should retain all morphological information of the object. That's why it is necessary to integrate a dynamic analysis of the object into a conventional framework of active stereoscopic systems. Figure 1 illustrates our 3D reconstruction approach based on iterative analysis of LSC of reconstructed 3D model.

At first, the projector projects a sparse regular spot pattern onto the object. By means of image processing tasks and a correspondence analysis the spatial point field can be derived. From all reconstructed 3D object points the surface is approximated by a Delaunay triangulation. The LSC at each 3D vertex/edge is then estimated, and a new pattern is created for the next iteration so that more points are projected in those areas with significant variation of surface curvature. The iterative process stops when the reconstructed 3D point cloud reflects the surface complexity as precise as expected; no human interaction is necessary.

The whole iterative process is described in details in the following paragraphs.

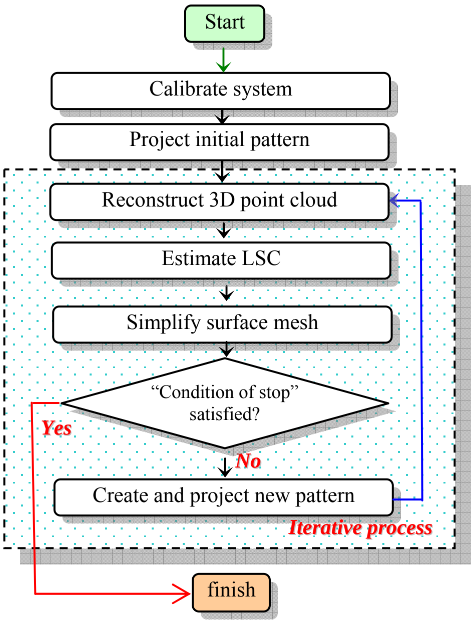

Figure 1: Iterative 3D reconstruction process

2.1 3D POINT CLOUD RECONSTRUCTION

After that the projector projects a certain point pattern onto the object, the stereopair takes a pair of images of the illuminated object (see figure 2). The image-based 3D point reconstruction process can be divided into 3 steps:

- Detection of 2D image point;
- 2D image point matching;
- Calculation of 3D object point coordinates.

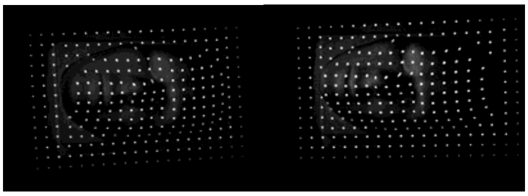

Figure 2: An example of images pair

2.1.1 Detection of 2D Image Point

In order to simplify and accelerate the detection process, the images are firstly pre-processed by generating gray-level image pyramids. The approximate location of each white spot is found out, and from the roughly detected spot position, we can easily get its pixel coordinates in the original image. The contour recognition technique is then applied to get the boundary of the spot. All pixels within the boundary are used for a weighted calculation of the COG to get the image coordinates of the spot. Sub-pixel precision is guaranteed by this image point detection method.

2.1.2 2D Image Point Correspondence

In 3D point reconstruction process, if the projected pattern points are not coded, it is impossible to assign directly a point in one image to a partner in the other image. Therefore, the correspondence problem has to be solved to determine, from a set of primitives in one image, the same set of primitives in another image [3].

Processing all points at the same time would be a very time-consuming task, since it needs to calculate the probability of correspondence between every point in image 1 and every point in image 2. If each image contains *n* points, this would mean *n!* comparisons. Thus, the algorithms runtime would grow exponentially when the number of points increases.

Since two corresponding points always lie on the same epipolar plane, we can use this constraint as a first filter to quickly reduce the number of possible candidates. Thus numerous unnecessary calculations are avoided, and the runtime grows linearly instead of exponentially with the number of points. Several methods are than applied to find out the most probable candidate among the remaining points. The two primary methods are: NLM (Nearest Line Method) and LEM (Local Elongation Method).

NLM makes further use of the epipolar geometry. Given a point *P* detected in image 1, a potential partner *P'* in image 2 must be situated on the epipolar line of *P* [4]. In practice, because of the impact of calculation errors such as the detected point positions, or the intrinsic and extrinsic parameters of the stereopair, *P'* may not be infinitely close to the epipolar line, but it should be very close. The search of a corresponding point can therefore be limited to the neighborhood of the epipolar line derived from the position in image 1. Based on approximate prior knowledge of the object, such as the size, the shape and the distance from the camera, the searching area can be reduced to a short segment of the epipolar line. If several candidate points are found in this searching space, the one which is nearest to the epipolar line is assigned the highest possibility. This method gives very good results, but depends highly on the quality of the prior knowledge.

LEM uses neighborhood information to reduce the searching area. For pattern points lying on the same straight line, if the object surface is relatively flat, their projections on the object should also be nearly on a same line. Therefore, a vector connecting two adjacent points whose corresponding points are already found out can be elongated to find the next point. As shown in figure 3, the green points have already been matched while the others not. The searching area in image 2 for the next neighbor point C is defined by the length and the directional angle of the vector BC. This method works very well for plane and curved areas, and the more points are already matched, the better is the result, because more vectors can be used to verify the correspondence. In case of breaks in the spatial shape of the object, the local surface continuity will be destroyed; the correctness of this algorithm can therefore be largely reduced. In this case, more constraints are applied, such as the relative position of two adjacent object points, or the probability of having major changes in the distance from the image to object [5].

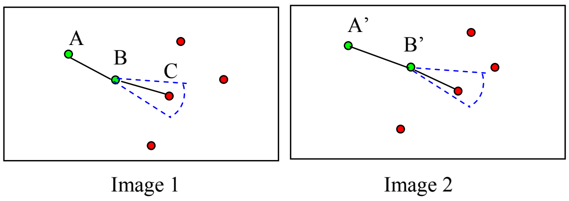

Figure 3: Searching area defined in LEM (Local Elongation Method)

2.1.3 Calculation of 3D Object Point Coordinates

From each pair of matched image points, the 3D coordinates of the corresponding object point can be calculated by ray intersection. The results of correspondence analysis can be verified by using the calibration information of the projector. Each reconstructed 3D point is transformed into the image space of the projector, and is compared to the real coordinates of the 2D pattern point. Since the maximum error of our projector calibration method does not exceed 2 pixels, all reconstructed 3D points showing larger differences tend to be incorrect and have to be eliminated.

2.2 LSC Estimation

Once the 3D point cloud is obtained, we generate a 3D surface mesh by a Delaunay triangulation. The Delaunay triangulation is generally unique. It has the property that the outcircle of every triangle does not contain any other point. The Delaunay triangulation is the dual structure of the Voronoi diagram [6].

From a theoretical point of view, triangular meshes do not have any curvature at all, since all faces are flat and the curvature is not properly defined along edges or at vertices because the surface is not C^2-differentiable. However, thinking of a triangular mesh as a piecewise linear approximation of an unknown smooth surface, the curvature of that unknown surface might be calculated using the information given by the triangular mesh itself [7]. Almost all the surface curvature estimation approaches proposed in the literature are based on vertices. Gaussian curvature is one of the most used.

In this section, we present 3 Gaussian curvature estimation approaches. Moreover, we propose a novel approach which is based on edges instead of vertices.

2.2.1 Gaussian Curvature Estimation

A normal curvature is the generalization of surface curvatures. Given a point P on the surface S and a direction $\vec{\tau}$ lying in the tangent plane of the surface S at P, the normal curvature is calculated by intersecting S with the plane spanned by P, the normal to S at P, and $\vec{\tau}$. The normal curvature is the signed curvature of this curve at P. If we compute the normal curvature for all values of $\vec{\tau}$ in the tangent plane at P, we will get a maximum value k_1 and a minimum value k_2 in two orthogonal directions. k_1 and k_2 are called principal curvatures.

The Gaussian curvature K (also called total curvature) and mean curvature H are differential invariant properties which depend only upon the surface's intrinsic geometry, and play a very important role in the theory of surfaces. They are defined as follow:

$$K = k_1 \times k_2\,, \qquad (2)$$

$$H = (k_1 + k_2) / 2. \qquad (3)$$

In our work, we chose the Gaussian curvature to evaluate the LSC, since for a minimal surface, the mean curvature is zero everywhere, whereas Gaussian curvature may vary in different zones; besides, the sign of Gaussian curvature gives extra information about the type of the local piecewise surface. A positive Gaussian curvature value means the surface is locally either a peak or a valley; a negative value means the surface locally has a saddle; and a zero value means the surface is flat in at least one direction (i.e., both a plane and a cylinder have zero Gaussian curvature) [8].

As we can see, the Gaussian curvature and mean curvature are defined only for twice differentiable (C^2) surfaces. To get 3D surface curvature information, different approaches have been proposed to estimate Gaussian and mean curvature [8,9,10]. Surazhsky *et al.* compared five curvature estimation algorithms, and drew a conclusion that the Gauss-Bonnet scheme is the best algorithm for the estimation of Gaussian curvature [10].

Vertex V_i is considered as a neighbor of vertex V if the edge VV_i belongs to the mesh. Denote the set of neighbors of V by $\{V_i \mid i = 1, 2, ..., n\}$, the set of triangles containing V by $\{T_i = \Delta\,(V_i, V, V_{(i+1)\ mod\ n}) \mid i = 1, 2, ..., n\}$, and the set of angles between V and its two successive neighbors by $\{\alpha_i = \angle\,(V_i, V, V_{(i+1)\ mod\ n}) \mid i = 1, 2, ..., n\}$ (see figure 4).

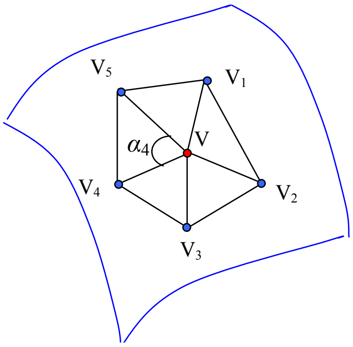

Figure 4: Surface patch approximated by small triangulates

In the literature, one of the most used Gauss-Bonnet based formula for estimation of Gaussian curvature K at vertex V is given in (4) [7, 11], where A_i is the area of triangle $\Delta\,(V_i, V, V_{(i+1) mod\ n})$.

$$K = \frac{2\pi - \sum_{i=1}^{n} \alpha_i}{\frac{1}{3} \sum_{i=1}^{n} A_i} \qquad (4)$$

As given in (5), instead of calculating the "real" area of each triangle, Meyer et al [12] consider that of Voronoi region of each triangle, denoted by A^{Mixed}.

$$K = \frac{2\pi - \sum_{i=1}^{n} \alpha_i}{\sum_{i=1}^{n} A_i^{Mixed}} \qquad (5)$$

A simpler approach can be applied by ignoring the areas of the triangles [8]:

$$K = 2\pi - \sum_{i=1}^{n} \alpha_i \qquad (6)$$

2.2.2 Our Approach

For continuous surface patch, the Gaussian curvature provides reliable information for our application. However, if a vertex has two neighbors on a same edge, and others on two planes, it has the value of zero (see figure 5). In this case, the Gaussian curvature is not appropriate for our application. We therefore proposed an approach based on edges for the analysis of the LSC.

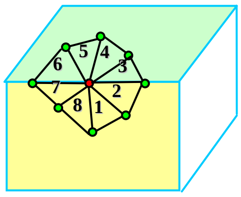

Figure 5: The type of surface patch for which Gauss-Bonnet scheme does not work.

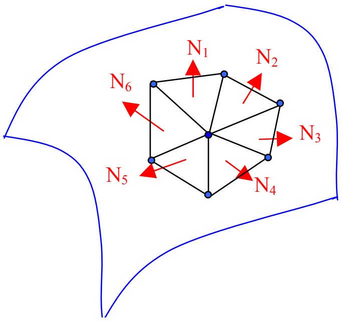

Figure 6: Analysis of LSC based on surface normal

As shown in figure 6, for each triangle, we can calculate its normal vector. The "normal vector" (often simply called the "normal") to a surface is a vector perpendicular to it. When normals are considered on closed surfaces, the inward-pointing normal (pointing towards the interior of the surface) and outward-pointing normal are usually distinguished. The normal vector is commonly denoted N. A plane which passes through 3 points $\{(x_i, y_i, z_i) \mid i = 1, 2, 3\}$ can be defined by the equation (7), where $N = [a \;\; b \;\; c]^T$ is the normal vector.

$$\begin{pmatrix} a & b & c \end{pmatrix} \begin{pmatrix} x_1 & x_2 & x_3 \\ y_1 & y_2 & y_3 \\ z_1 & z_2 & z_3 \end{pmatrix} = \begin{pmatrix} 1 & 1 & 1 \end{pmatrix} \qquad (7)$$

The angle θ between two intersecting planes is known as the "dihedral angle". If we define the two planes by the equation (8) and (9), their normal vectors are respectively $N_1 = [a_1 \;\; b_1 \;\; c_1]^T$ and $N_2 = [a_2 \;\; b_2 \;\; c_2]^T$. The dihedral angle between the two planes is given via the dot product of the two normals as in (10), and we define the LSC at the intersection of two planes as in (11).

$$a_1 x + b_1 y + c_1 z = 1 \qquad (8)$$

$$a_2 x + b_2 y + c_2 z = 1 \qquad (9)$$

$$\cos\theta = N_1 \bullet N_2$$

$$= \frac{a_1 a_2 + b_1 b_2 + c_1 c_2}{\sqrt{a_1^2 + b_1^2 + c_1^2}\sqrt{a_2^2 + b_2^2 + c_2^2}} \qquad (10)$$

$$K = \theta \qquad (11)$$

2.3 Mesh Simplification & Pattern Adaptation

As described previously, at the end of each iteration, a 3D triangular surface mesh is obtained. Depending on the LSC estimation approach chosen by the user, each vertex or edge of the 3D mesh is evaluated. By comparing the values to the two pre-defined thresholds τ_1 and τ_2, respectively expressing “low” and “high” LSC, the vertex might be eliminated to simplify the mesh, or be selected as a candidate for new pattern generation. If no such candidate is obtained, then the iterative process stops; otherwise, a new pattern is generated and then projected on the object, and the process continues.

In the following paragraphs, we explain how the mesh is simplified and how to create the new pattern in different cases, and how to project the new pattern if the points are too dense.

2.3.1 Mesh Simplification

Since our objective is to obtain an optimized 3D model, the reconstructed 3D points which have “low” LSC are removed from the 3D model before the next iteration begins. According to the applied LSC estimation approach, “low LSC” is interpreted differently.

For the Gaussian-curvature-based LSC approach, a given vertex V is regarded as having “low” LSC if the value of K is inferior to τ_1.

In case of our edge-based LSC approach, all neighbors of a vertex V have to be studied to verify if the assumption of “low” LSC is correct. We calculate therefore the maximum dihedral angle $\theta_{\max}$ between every pair of adjacent triangles, if the value of $\theta_{\max}$ is inferior to τ_1, then V is thought as having “low” LSC.

2.3.2 New Patten Generation

At first, an image with black background is created, and then all calculated new pattern points are added into the image according to their image coordinates. Two methods of calculation of new pattern points are provided.

2.3.2.1 New Patten Generation based on Gaussian Curvature Estimation Approaches

A vertex V of the current 3D triangular mesh will be selected as candidate vertex for new pattern generation only if all of the following conditions are satisfied:

- Its LSC K is superior to τ_2 ;
- V is not situated at the board of the surface mesh;
- The area of each triangle is superior to the pre-defined threshold *minTriArea* (ex., 3 mm^2).

For each candidate vertex V, four new pattern points are added in the list of new pattern points. The positions of these points are determined in two steps: Firstly, the corresponding pattern points of the vertex V and all its neighbors are found out by using the calibration matrix M (see section 2.2); and secondly, the value

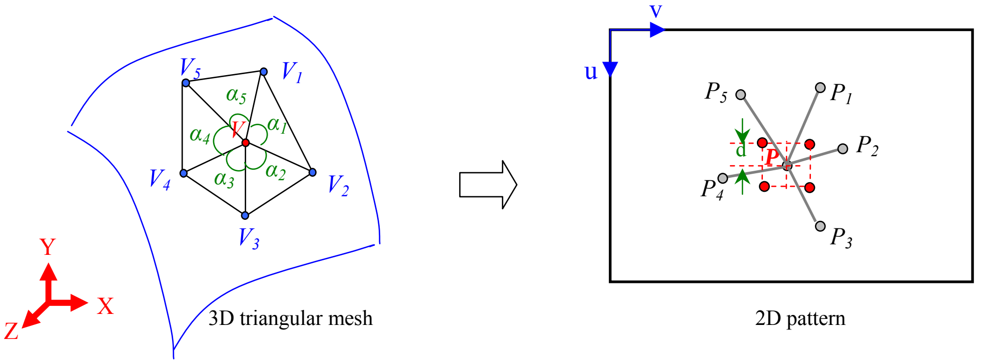

Figure 7: four pattern points are added in new pattern around the position of old pattern point P.

of d is determined (see figure 7). Since the density of the 3D point cloud increases progressively after each iteration, the value of d has to be adapted to the current 3D mesh. We therefore set the value of d as $d = r \times D$, where D is the average distance between the vertex V and all its neighbors in the current 3D mesh, and r is a ratio pre-configured by user, it can be 1/2, 1/3, 1/4, etc.

2.3.2.2 Patten Adaptation Based on Our Surface Curvature Approach

An edge E of the current 3D triangular mesh will be selected as candidate edge for new pattern generation only if the two following conditions are both satisfied:

- Its LSC K is superior to τ_2;
- The area of each triangle is superior to the pre-defined threshold *minTriArea* (ex., 3 mm^2).

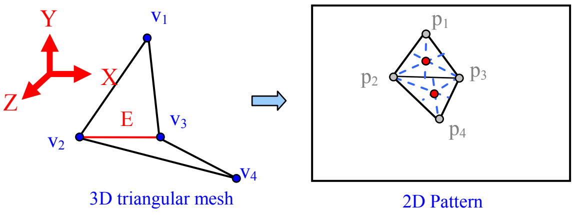

Figure 8: Determination of positions of new pattern points from a 3D edge which has high surface curvature.

For each candidate edge E, as shown in figure 8, the corresponding pattern points of the four vertices of the two adjacent triangles are determined by using the calibration matrix M, and then a new pattern point will be added at each Triangle Centroid (in red).

2.3.3 New Pattern Projection

By analyzing the LSC of each vertex / edge of the current 3D surface mesh, an adapted pattern is generated. Figure 9 shows an example of pattern at the 3rd iteration during the 3D reconstruction process. The pattern will be divided into several sub-patterns so that in the acquired images, the distance between whichever two adjacent points is big enough to simplify the 2D image points matching problem.

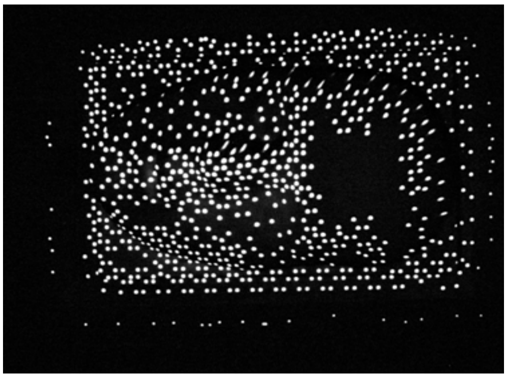

Figure 9: An example of modified pattern at the 3rd iteration, for the 3D reconstruction of a mask.

3. RESULTS

Numerous experiments have been made on different types of objects. In this section, we present the reconstruction results for a blue plate (length: 200mm, width: 150mm, depth: 50mm) and a gray mask (length: 200mm, width: 140mm, depth: 120mm), as shown in figure 10.

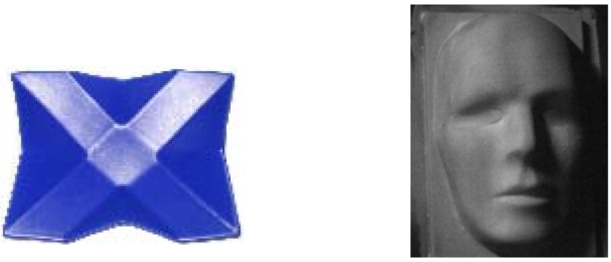

Figure 10: Two objects to be reconstructed: blue plate and gray mask.

For each object, the four LSC estimation approaches were applied one by one. The reconstruction results of the plate are summarized and compared with the reference model M_{ref} in table 1, and visualized in figure 9. M_{ref} was obtained by using a professional fringe projection system (GOM Atos II). M_{ref_simp} is the simplified model of M_{ref} by using the mesh simplification tool furnished by the system. The mesh simplification is done by minimizing an energy function and eliminating uniformly vertices from the original 3D mesh. As for the three models obtained by applying the LSC estimation approaches described by formula (4), (5) and (6) in the section 2.2.1, they are named respectively M_{GC1}, M_{GC2}, M_{GC3}. The model issued from our approach is named as M_{LI}.

	M_{ref}	M_{ref_simp}	M_{GC1}	M_{GC2}	M_{GC3}	M_{LI}
Number of points	96,194	4,817	1,494	1,814	1,823	2,031
Standard deviation vs. M_{ref} (mm)	-	0.34	0.68	0.36	0.61	0.08

Table 1: Comparison of reconstruction results of the blue plate.

The data in table 1 indicate that compared to M_{ref}, M_{LI} has the smallest standard deviation: 0.08, which is three times smaller than that of M_{ref_simp} vs. M_{ref}. Moreover, M_{LI} contains only 2,031 points, compared to M_{ref_simp}, the number of points was reduced 58%.

From figure 11, we can see that the simplified reference model M_{ref_simp} is represented by a point cloud which lies almost uniformly on the surface, even in flat areas. As for M_{LI}, however, it contains very dense points around the creases, but hardly any point in flat areas.

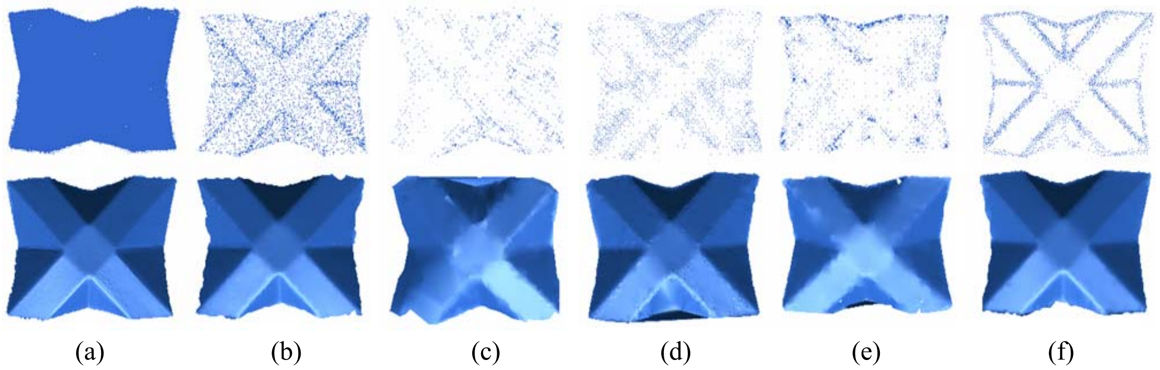

Figure 11: Comparison of reconstruction results of the blue plate, each described respectively by 3D point cloud and shaded 3D surface mesh. (a) M_{ref}; (b) M_{ref_simp} ; (c) M_{GC1} ; (d) M_{GC2} ; (e) M_{GC3} ; (f) M_{LI} .

Figure 12 shows two standard deviation maps. They were obtained by comparing respectively M_{ref_simp} vs. M_{ref}, and M_{LI} vs. M_{ref}. Obviously, the quality of our 3D model M_{LI} is better, since it has low deviation (represented by blue color) everywhere, whereas the commercial one M_{ref_simp} is covered by colors which represent higher deviation, especially around the creases and the edges.

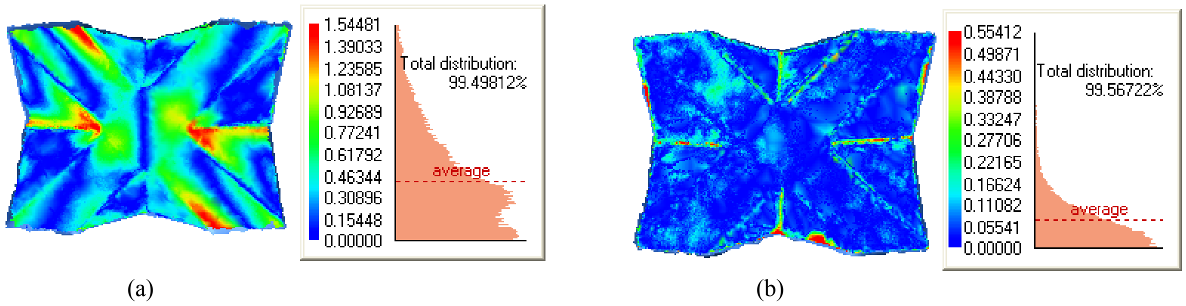

Figure 12: Comparison of simplified meshes. (a) model deviation map between M_{ref_simp} and M_{ref} (standard deviation: 0.34mm); (b) model deviation map between M_{LI} and M_{ref} (standard deviation: 0.08mm).

Considering the above factors, we can regard that model M_{LI} is the best optimized 3D model. Figure 13 gives some reconstruction results of the plate at each iteration, it is easy to notice that the projected pattern points fell closer and closer to the creases and the edges of the plate after each iteration, and that after the second iteration, extremely less points were projected in flat areas.

As shown in table 1 and figure 11 (d), the LSC estimation approach expressed in formula (5) in section 3.2.1 gave also good result: the obtained 3D model has almost the same standard deviation as the one obtained by commercial mesh simplification tool, and the number of points was reduced 62%. However, compared to our LSC estimation approach, those Gaussian-curvature-based approaches gave worse results. The reason was illustrated by figure 13 in section 3.2.2., showing that the variation of the surface curvature around a vertex is measured more precisely because all directions are taken into account. In the given example, the candidate vertex has 8 neighbours and a non-uniform curvature distribution. By applying our LSC estimation approach, new pattern points will be projected in the triangles 2, 3, 6 and 7, which allows achieving more rapidly the surface information around the edge; In the case of Gaussian-curvature-based approach, however, it is hard to project precisely new points near the creases or the edges, because of its averaging characteristic. As result, some points will be projected uselessly in flat areas.

For objects with continuous surface curvature variations, by applying the Gaussian-curvature-based LSC estimation approaches, the quality of obtained 3D models is much better, but still not as good as that obtained by our LSC estimation approach.

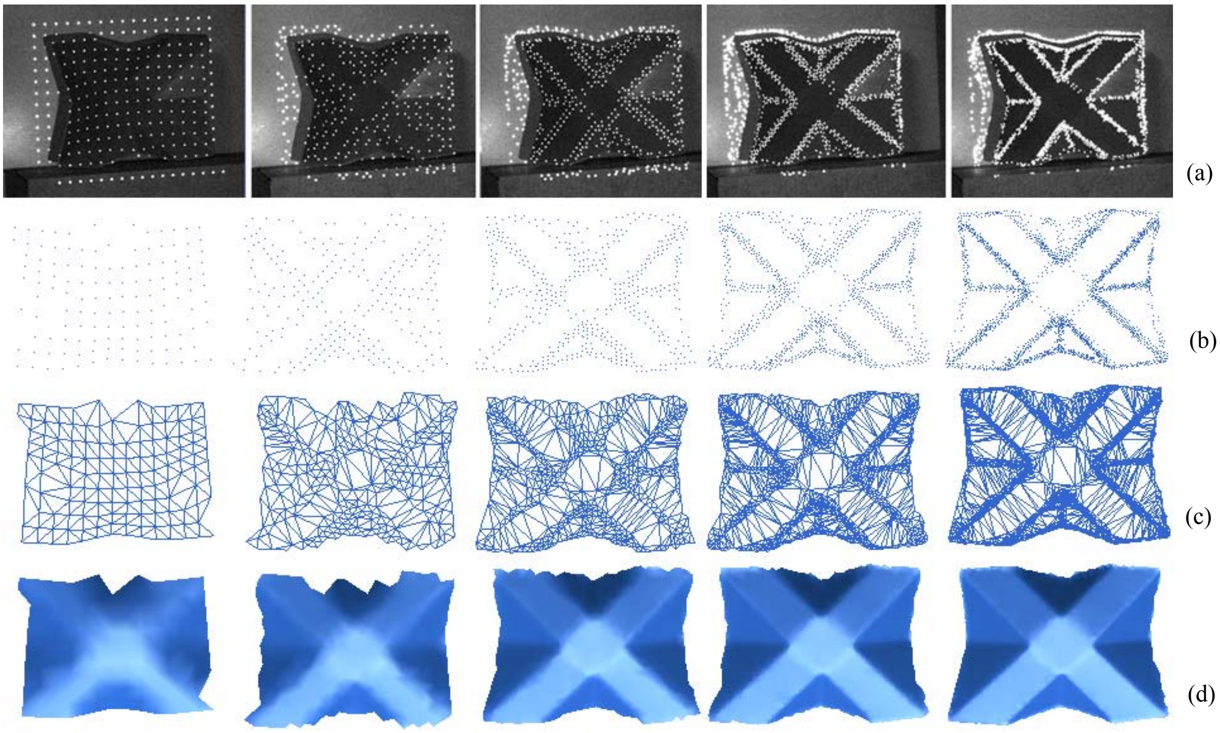

Figure 13: 3D reconstruction results of the blue plate at iteration 1 ~ 5, obtained by applying our LSC estimation approach, described respectively by each column. (a) the projected pattern at each iteration; (b) the 3D point clouds. 1st Iteration: 132 points, 2nd iteration: 261 points, 3rd iteration: 517 points; 4th iteration: 1,076 points, 5th iteration: 2,031 points; (c) the obtained 3D surface meshes; (d) Shaded surface meshes.

4 CONCLUSIONS

We presented a newly close range stereo-photogrammetry system which is based on iterative and adaptive pattern projection. The objective is to restrict data capture to characteristic surface areas during the image acquisition process, thus the reconstructed 3D model will be ensured to be fitted to the morphology of an object. The system projects iteratively spot patterns adapted to the object surface geometry. At each iteration, we calculate the local surface curvature for each vertex or edge of the actual 3D mesh, and decide where to project more points at the next iteration.

Numerous experiments were made on objects with different types of surface, and it was proved that our system is capable to reconstruct 3D models with high precision. By applying our edge-based LSC estimation approach, optimized 3D models can be achieved, containing much fewer points compared to those ones obtained by a professional fringe projection system GOM Atos II, whereas all important morphological information about the object's surface was captured.

The reason why our approach provides better optimized 3D models lies on the fact that the caption of characteristic surface information is controlled during the acquisition process. We begin with a rough 3D model, and the significant areas are localized more and more precisely, so that the 3D model is refined progressively in these areas. As to most of the mesh simplification approaches proposed in the literature, however, they usually consist of removing progressively points from a very dense 3D point cloud by minimizing an energy function. The disadvantage is that in this case, the surface curvature is less reliable as indicator weather a point is situated in a significant area, because the neighbourhood of a given point is extremely close, and such a small piece of surface patch has the tenancy to be flat, even if it is part of a characteristic surface area.

Currently, the pattern control is only based on LSC estimation, because the geometry of the object is totally unknown before the 3D reconstruction begins. Our future work will therefore focus on the integration of *a priori* knowledge about the object into our system. By combining the *a priori* knowledge and the LSC estimation, the system would be able to localize rapidly the areas which interest the most the user, so that more precise capture would be realized for these areas. Such an approach can be applied into some industrial applications, such as quality control.

REFERENCES

[1] H. Hoppe, T. DeRose, T. Duchamp, J. McDonald, W. Stuetzle, Mesh optimization, in Proceedings of the 20st Annual Conference on Computer Graphics and Interactive Techniques, SIGGRAPH 1993, 1993, pp 19-26.

[2] W. Li, F. Boochs, F. Marzani, Y. Voisin, Iterative 3D surface reconstruction with adaptive Pattern projection, in Proc. of the Sixth IASTED International Conference on Visulatization, Imaging and Image Processing (VIIP), Palma De Mallorca, Spain, 2006, pp.336-341.

[3] J. Battle, E. Mouaddib, J. Salvi, Recent progress in coded structured light as a technique to solve the correspondence Problem: a Survey, Pattern Recognition, 1998, 31(7), pp. 963-982.

[4] O.Ghita, J.Mallon, P.F.Whelan, Epiploar line extraction using feature matching, In Proc. Irish Machine Vision and Image Processing Conference 2001, NUI Maynooth, 2001, pp 87-95.

[5] M. Böhler, F. Boochs, Getting 3D shapes by means of projection and photogrammetry, Inspect, GIT-Verlag, Darmstadt, 2006.

[6] S. Kanaganathan, N.B. Goldstein, Comparison of four point adding algorithms for Delaunay type three dimensional mesh generators, IEEE Transactions on magnetics, 1991, 27(3).

[7] N. Dyn, K. Hormann, S.J. Kim, D. Levin, Optimizing 3D triangulations using discrete curvature analysis, Mathematical Methods for Curves and Surfaces, Oslo 2000, Nashville, TN., 2001, pp.135-146.

[8] L. Alboul, G. Echeverria, M. Rodrigues, Discrete curvatures and gauss maps for polyhedral surfaces, in European Workshop on Computational Geometry (EWCG), Eindhoven, the Netherlands, 2005, pp. 69–72.

[9] J. Peng, Q. Li, C.C. Jay kuo, M. Zhou, 2003. Estimating Gaussian Curvatures from 3D meshes. SPIE Electronic Image, vol.5007, pp. 270-280.

[10] T. Surazhsky, E. Magid, O. Soldea, G. Elber, E. Rivlin, A comparison of gaussian and mean curvatures estimation methods on triangular meshes, in IEEE International Conference on Robotics & Automation, 2003.

[11] J.-L. Maltret, M. Daniel, Discrete curvatures and applications: a survey. Rapport de recherche 004.2002, Laboratoire des Sciences de l'Information et des Systèmes, 2002.

[12] M. Meyer, M. Desbrun, P. Schröder, A.H. Barr, Discrete differential-geometry operators for triangulated 2-manifolds, In Proc. VisMath 02, Berlin, Germany, 2002, pp.35-57.

Prof Dr. Frank Boochs received his PhD in geodesy from the institute of photogrammetry, university of Bonn in 1984. Since 1993 he is with the university of applied sciences, Mainz. He is head of the Institute for Spatial Information and Surveying Technology there.

His interests are in the field of digital image matching techniques,image analysis, digital sensor technology, data collection for geographic information systems and software engineering. He is also head of the computer vision group of the german society for photogrammetry, remote sensing and geoinformation.